OPEN ACCESS

ACTA METALLURGICA SLOVACA

2025, VOL. 31, NO. 3, 186-193

SCICELL

RESEARCH PAPER

Enhanced Shear Deformation in Rod Rolling with Inclined Oval Pass Modification

Kairosh Nogayev[1], Maxat Abishkenov[1], Ilgar Tavshanov[1], Zhassulan Ashkeyev[1], Vyacheslav Kunaev[1], Gulzhainat Akhmetova[2], Aman Kamarov[1]*

[1]Karaganda Industrial University, Department of Technological Machines and Transportation, Republic Avenue 30, Temirtau 101400, Kazakhstan
[2]Karaganda Industrial University, Department of Metallurgy and Materials Science, Republic Avenue 30, Temirtau 101400, Kazakhstan

*Corresponding author: k.nogayev@tttu.edu.kz, tel.: +7 7004109176, Department of Technological Machines and Transportation, Karaganda Industrial University, Republic Avenue 30, Temirtau 101400, Kazakhstan

Received: 14.08.2025
Accepted: 20.08.2025

ABSTRACT

This study presents a novel approach for implementing intense shear deformation in rod rolling by modifying the traditional oval–round pass design. The proposed scheme utilizes oval passes with an inclined longitudinal axis to induce skew-symmetric rolling conditions that generate enhanced shear deformation. Analytical models were developed to determine the roll grip length for the new geometry, and numerical simulations using DEFORM 3D were carried out to assess stress–strain distribution and plastic flow behavior. Laboratory experiments were performed on 25G2S structural steel using both the classical and new rolling schemes. The results demonstrated that the inclined pass configuration not only increases the overall strain intensity and homogeneity but also improves the mechanical properties of the final product. In particular, the new scheme enhanced ductility without compromising strength, partially mitigating the well-known strength–ductility trade-off. These findings highlight the potential of the proposed rolling method for industrial applications in improving metal quality.

Keywords: rolling; severe plastic deformation; oval-round pass design; stress-strain state; finite element method; numerical analysis; experimental validation.

INTRODUCTION

In modern continuous workpiece and rod rolling mills, the most commonly used pass sequence is round-oval-round [1-3]. However, such a scheme has some disadvantages associated with the inhomogeneity of deformation in the radial and circumferential directions of the workpiece, which leads to corresponding heterogeneities in the mechanical properties along the cross-section [4]. In addition, with each pass in this sequence, the level of damage increases, particularly near the surface, leading to the formation of voids [5]. The main limitation of classical oval passes in the oval-round sequence is the relatively low elongation factor, which prevents the achievement of the required final dimensions of the rod and limits the effectiveness of eliminating defects in the original cast workpiece [6].

To overcome these limitations, severe plastic deformation (SPD) methods have been actively investigated in recent years, enabling the achievement of significant deformations without substantial changes in the overall dimensions of the workpiece [7-9]. The key difference between SPD and traditional methods is the high proportion of shear components in the overall deformation process, which promotes the intensification of the hardening and grain refinement processes [10-12].

One promising direction for SPD application under rolling conditions is the use of special passes, which provide a combination of high-altitude reduction and transverse shear. Thus, [13-15] demonstrated the effectiveness of the non-diagonal arrangement of rhombic passes, in which counter-current plastic flows with opposite vectors are formed in the deformation zone, thereby generating intense shear deformations. Numerical and experimental studies have demonstrated that combining these deformations enhances the micromechanical properties of metals, including strength and structural homogeneity.

The possibility of adapting the concept of a non-diagonal arrangement of rhombic passes for oval passes in the oval-round sequence is a viable research direction that warrants exploration. Implementing intense shear deformations in oval passes can contribute to a more efficient elimination of defects in cast workpieces, increase the uniformity of mechanical properties across the cross-section, and improve the performance characteristics of the final products. Thus, the integration of SPD principles into traditional rolling schemes opens new perspectives for enhancing the pressure metal treatment technology.

MATERIAL AND METHODS

Principles of Implementing Intense Shear Deformations in Oval Passes

Let us arrange the axes of symmetry of the oval in the passes obliquely relative to the roll axis to implement intense shear deformations in the oval passes (**Fig. 1**). Here, transverse shear occurs in the deformation zone simultaneously with high-altitude reduction, which provides a higher level of shear deformation than rolling in the classical oval passes.

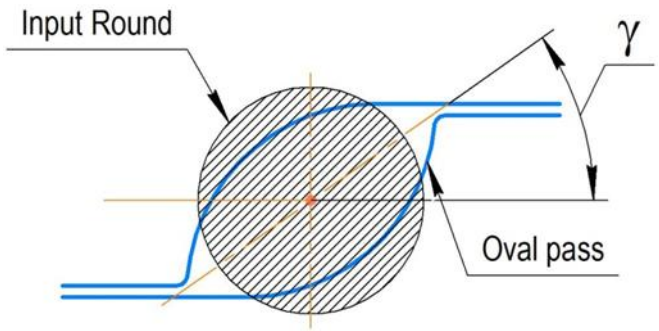

Fig. 1 Pass with inclined oval arrangement

Let us perform the alternating macro-shift deformation in four passes in the oval-round pass sequence, forming one cycle, as shown in **Fig. 2**.

The first pass. The initial round workpiece was set as an oval pass with an inclined oval arrangement. In the deformation zone, the workpiece is subjected to intense shear deformation in the transverse direction owing to the skew-symmetric impact of the upper and lower rolls and high-altitude reduction.

The second pass. The initial breakdown with an oval cross-section is rolled in the round pass using the classical method, that is, the oval initial breakdown is set in the round pass by the longer axis of the oval symmetry perpendicular to the longitudinal axis of the rolls by tilting at an angle of 90°– γ (where γ is the angle of inclination of the longer axis of the oval symmetry relative to the longitudinal axis of the rolls). Metal deformation in a round pass is mainly performed by a high-

altitude reduction in thickness and limited widening through the separation of the plastic displacement flow relative to the vertical axis of pass symmetry.
The third pass. The initial breakdown with a round cross-section is set into an oval pass with an inclined oval arrangement, where, in contrast to the pass in the first passage, the axes of symmetry of the oval are inclined in the opposite direction relative to the longitudinal axis of the rolls. Here, the sign of the shear deformation was reversed relative to the sign of the shear deformation in the first pass.
The fourth pass. The oval initial breakdown was tilted at an angle of 90°– γ (**Fig. 2**) and rolled in the oval pass according to the classical scheme.

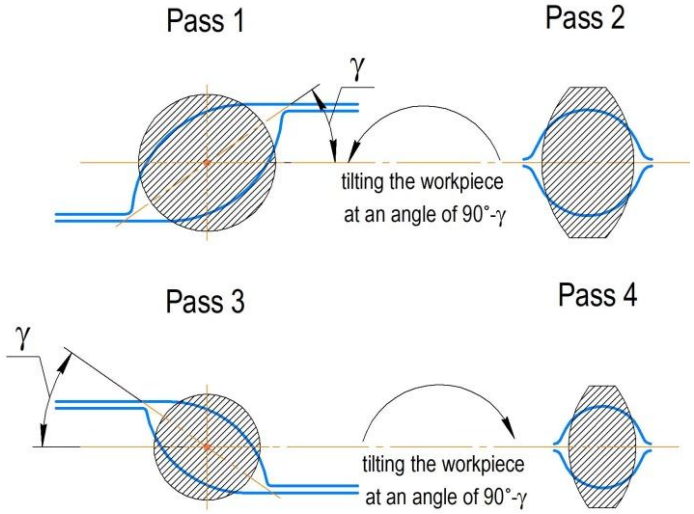

Fig. 2 A new rolling scheme in an alternating paired sequence of "oval-round" passes

Analytical Determination of Roll Grip Length for Rolling in Inclined Oval Passes

Different studies [1, 2, 16] have determined the maximum roll grip length for the classical oval pass. These studies provided expressions for determining the maximum roll grip length when the radius of the roll circle along the plane of the oval pass changed symmetrically relative to the symmetry axis of the oval pass. In this case, the contact point of the workpiece with the roll, which is the most distant from the plane of the oval pass, determines the maximum roll grip length and is in the vertical medial plane of the oval pass. In our case, the change in the circular radius of the roll along the plane of the oval pass was asymmetrical relative to the symmetry axis of the oval. Therefore, the expressions for determining the maximum grip length given in the abovementioned studies are not suitable for rolling inclined oval passes.
To determine the grip length for rolling in inclined oval passes, let us consider the intersection of the roll with a round workpiece without considering widening. We assumed an *XYZ* coordinate system, where the origin, *O* was in the pass plane at the intersection of the symmetrical axes of the oval. **Fig. 3** shows a diagram explaining the roll grip in inclined oval passes, where the medial plane of the oval pass is denoted by $P_{s.ov.}$ The plane of the contact point between the workpiece and the roll passing through the *Z*-axis and maximally distant from the plane of the oval pass is denoted as P_L.
The grip length can be determined from the expression of the points of intersection between the roll circle and original workpiece circle. Let us consider the diagram shown in **Fig. 4** to obtain the expression.
With the adopted *XYZ* coordinate system, let us write the equation of the circles in the following form:
- For the round workpiece circle:

$$x^2 + y^2 = r_0^2 \tag{1}$$

- For the roll circle:

$$z^2 + (y - R)^2 = R_r^2 \tag{2}$$

where: r_0 is the radius of the round workpiece circle;
R is the distance from the rolling line to the roll axis;
R_r is the radius of the roll circle.

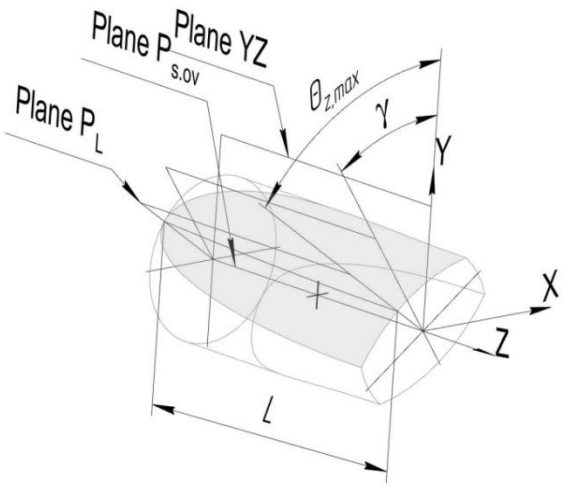

Fig. 3 Diagram of workpiece gripping by rolls during rolling in inclined oval passes

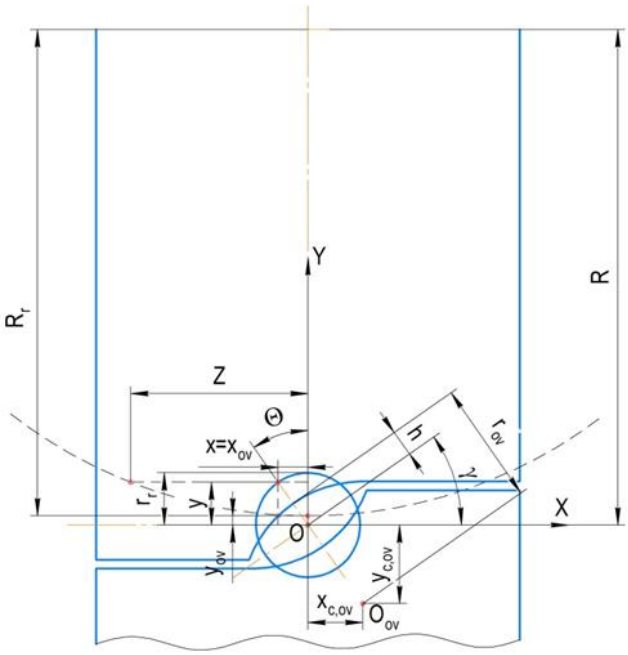

Fig. 4 Diagram for obtaining the expression of the intersection points of the roll circles with the circle of the original workpiece

We express the values of *x* and *y*, which determine the position of the intersection point of the circles of the roll and the round workpiece, through the angle θ:

$$y = r_0 \cdot \cos\theta \tag{3}$$

$$x = r_0 \cdot \sin\theta \tag{4}$$

where: θ is the angle between the YZ-plane and the plane passing through the Z-axis and the intersection point of the circles of the roll and the round workpiece.

From Equation (2) and considering Equation (3), we obtain an expression that determines the distance from the intersection point of the circles of the roll and the round workpiece to the plane of the pass:

$$z = \sqrt{R_r^2 - (R - r_0 \cdot \cos\theta)^2} \quad (5)$$

The radius of the roll circle is determined using the following equation:

$$R_r = R - y_{ov} \quad (6)$$

where: y_{ov} is the coordinate of the intersection point of the line of the oval with the roll circle plane along the *Y* axis.

To determine y_{ov}, let us make an equation of the line of the oval, representing it by the arc of a circle centered at point O_{ov}:

$$(x_{ov} - x_{c.ov})^2 + (y_{ov} - y_{c.ov})^2 = r_{ov}^2 \quad (7)$$

where: x_{ov} is the coordinate of the intersection point of the line of the oval with the roll circle plane along the *X* axis;
$x_{c.ov}, y_{c.ov}$ are coordinates of the curvature center of the oval;
r_{ov} is the curvature radius of the oval.

The value of x_{ov} is determined from Equation (4) because the position of the plane of the roll circle also determines it.
From the diagram in **Fig. 4**, while tilting the oval pass by an angle γ, we determine the values of the coordinates of the curvature center of the oval:

$$x_{c.ov} = (r_{ov} - h) \cdot \sin\gamma \quad (8)$$

$$y_{c.ov} = (h - r_{ov}) \cdot \cos\gamma \quad (9)$$

where: h is half the height of an oval pass.

Given Equation (6), let us write Equation (5) in the form:

$$z = \sqrt{(R - y_{ov})^2 - (R - r_0 \cdot \cos\theta)^2} \quad (10)$$

where: we substitute y_{ov} from the following equation obtained from Equation (7) considering Equations (4), (8) and (9):

$$y_{ov} = \sqrt{r_{ov}^2 - [r_0 \cdot \sin\theta - (r_{ov} - h) \cdot \sin\gamma]^2} + (h - r_{ov}) \cdot \cos\gamma \quad (11)$$

The maximum grip length *L* is equal to the maximum value of z_{max}, which can be calculated from Equations (10) and (11) by changing the value of angle θ. The angle between the *YZ* plane and the P_L plane we denoted as $\theta_{z.max}$.

Modeling of the Rolling Process in Classical and Inclined Oval Passes

The features of the new method were tested by modeling the rolling process using the DEFORM 3D software package [17-19]. The problems of hot rolling of a workpiece in a classical oval pass and inclined oval pass were simulated.
The following assumptions and simplifications were adopted when setting the modeling problems:
- The working tool is a rigid body with constant temperature;
- The rolled material is homogeneous and isotropic;
- The deformable medium used is viscoplastic.

The billet material used in the rolling simulation was AISI-1045 steel from the standard DEFORM-3D library, whose rheological model is specifically developed for simulating hot deformation in the 900–1200 °C range. AISI-1045 was chosen for its robust rheological modeling foundation and representative characteristics, ensuring that our findings remain broadly applicable to analogous structural steels under hot rolling conditions. The process temperature was 1200 °C. A finite element mesh with 86168 elements of deformable workpiece was generated to ensure calculation accuracy. The friction condition between tools and the workpiece was modeled using the Siebel (constant-shear) friction law with a friction factor 0.7, as generally recommended for hot, dry forming operations in DEFORM-3D. The kinematic parameters of the simulation and the geometric characteristics of the pass were selected according to the specifications of the laboratory rolling mill stand, which was subsequently used for the experimental rolling described in the following subsection. Accordingly, the rotation of the deforming tools was set to 1.0472 rad/s. **Fig. 5** shows the dimensions of the initial circle and the pass.

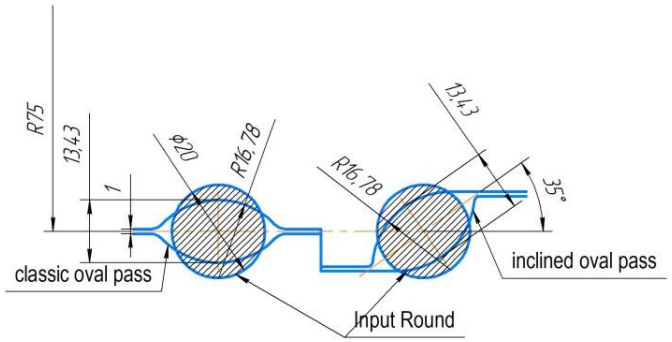

Fig. 5 Dimensions of the initial circle and the pass

Experimental Procedure for Validation of the Rolling Scheme

To validate the feasibility of the proposed "oval–round" rolling sequence with inclined oval passes and to evaluate its effect on the mechanical properties of the rolled products, a series of laboratory rolling experiments was conducted.
For the rolling experiments, special rolls were manufactured for installation on the laboratory rolling mill stand, as shown in **Fig. 6**. The roll design incorporated both classical and inclined oval passes, allowing for a comparative analysis of their effects (**Fig. 7**).
The initial workpieces were prepared from 25G2S structural steel, a low-alloy steel grade regulated by the Russian standard GOST 5781-82 and the Bulgarian standard BDS 4758, in the form of cylindrical billets with a diameter of 20 mm and a length of 150 mm.
Rolling was performed in four passes using two different sequences: the classical and the newly proposed "oval–round" configuration with inclined oval passes. The elongation ratio in each pass was set to 1.3. According to the laboratory rolling stand's specifications, the roll rotation speed was fixed at 1.0472 rad/s for all passes. The rolling process resulted in final round bars with a diameter of 12 mm.

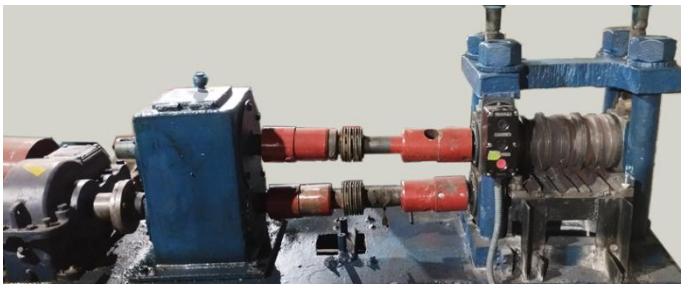

Fig. 6 Laboratory rolling mill stand

To evaluate the mechanical properties of the rolled products, standard specimens were machined from the final bars. Tensile tests were performed according to ISO 6892-1 using a WDW-100 electromechanical universal testing machine with a maximum load capacity of 100 kN. The geometry and dimensions of the tensile specimens, as well as their appearance, are illustrated in **Fig. 8**. The tests were conducted at a constant crosshead speed of 1.5 mm/min, in accordance with the recommendations outlined in [20].

RESULTS AND DISCUSSION

Influence of Oval Pass Inclination on the Geometry of the Deformation Zone

Checking the correctness of the expressions involved the calculation of z sub m a, x, and theta sub z z_{max} and $\theta_{z.max}$ values using the brute force search method [21] on a uniform mesh of θ values in the range of $-1.57 \le \theta \le 0$ rad. ($-90° \le \theta \le 0°$) and the comparison of the obtained values with the results of the geometric 3D modeling using CAD program for $r_0 = 14.75$ mm, $r_{ov} = 34.5$ mm, $h = 7.4$ mm, $\gamma = 35° = 0.610865238$ rad., $R = 140$ mm. As a result, we obtained $z_{max} = 52.24282$ mm at $\theta_{z.max} = -0.964945$ rad. ($-55.2873°$). The geometric 3D modeling of the workpiece gripping by the roll shown in **Fig. 9** provides the same values of z_{max} and $\theta_{z.max}$ for the given values of r_0, r_{ov}, h, γ, and R, which

confirms the correctness of the derivation of the expression for determining the maximum roll grip length when rolling in the inclined oval pass.

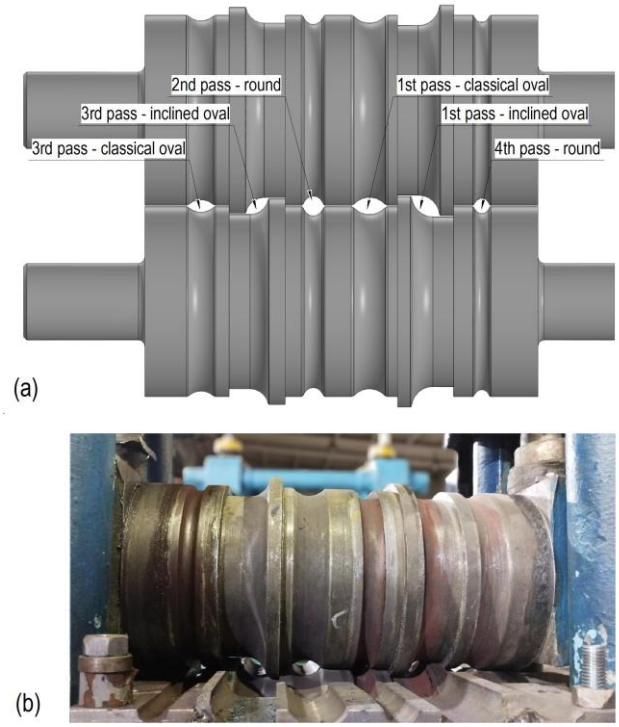

Fig. 7 Design of the roll with combined classical and inclined oval passes (a) and installation of the roll in the laboratory stand (b)

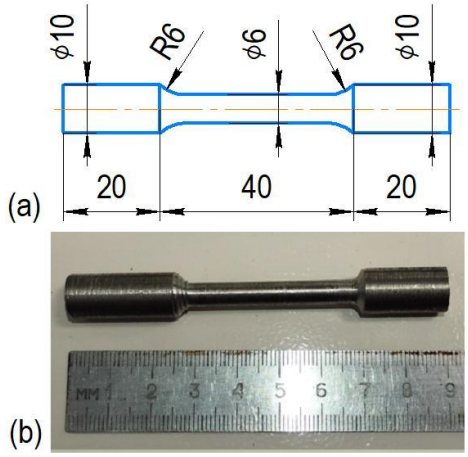

Fig. 8 Geometry and dimensions of the tensile specimen (a) and photograph of the prepared sample (b)

It is worth noting that at $\gamma = 0°$ from Equations (10) and (11), we can obtain the expression for the maximum grip length for the classical oval pass. Here, $\theta_{z.max} = 0$ because the contact point of the workpiece with the roll was in the vertical medial plane of the oval pass. Subsequently, for the classical oval pass, we obtain the following:

$$L = z_{max} = \sqrt{(R-h)^2 - (r_0 - R)^2} \tag{12}$$

or

$$L = \sqrt{2 \cdot R \cdot (r_0 - h) + h^2 - r_0^2} \tag{13}$$

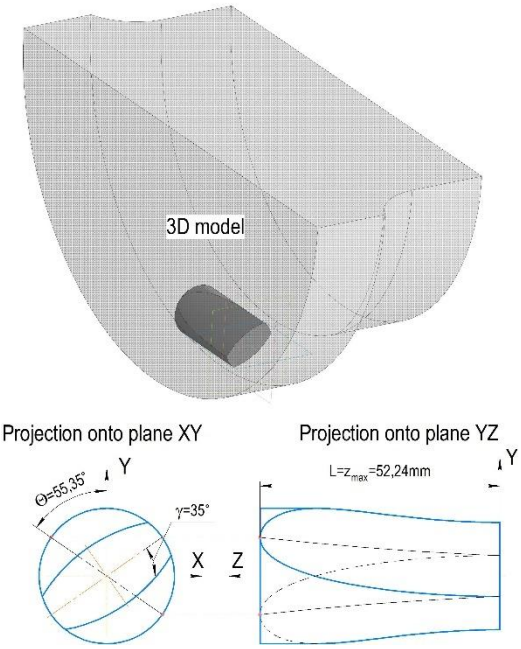

Fig. 9 Geometric 3D modeling of workpiece gripping by roll using CAD program

The identification of the inclination angle γ influence on the maximum grip length L and the deviation of the planes $P_{s.ov}$ and P_L involved solving expression (10) and determining the values of z_{max} and $\theta_{z.max}$ at different values of the angle γ. The values of r_0, r_{ov}, h, and R for the calculations were the same as those in the previous calculation. According to the calculation results, **Fig. 10** shows the graph of $z(\theta)$ dependence for different values of angle γ, and **Table 1** presents the obtained values of z_{max} and $\theta_{z.max}$.

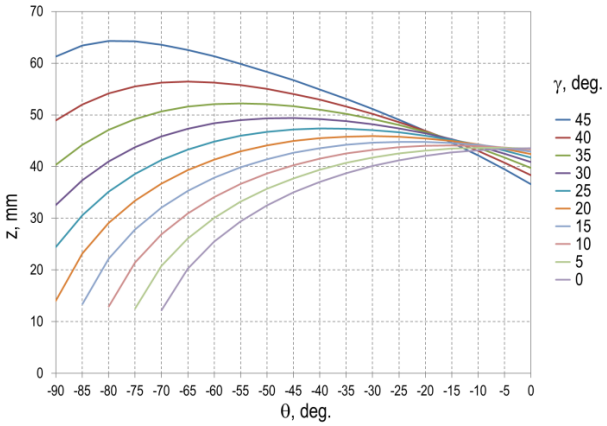

Fig. 10 Graph of *z(θ)* dependence on different values of angle γ

The results of the numerical calculations showed an increase in the absolute values of $\theta_{z.max}$ as the inclination angle of the oval pass γ increased. This indicates that plane P_L, passing through the contact point, which is maximally distant from the plane of the oval pass, deviates more from the vertical plane *YZ* compared to the medial plane of the oval pass. This indicates the formation of a skew-symmetric impact from the upper and lower rolls during rolling in the inclined oval passes. The skew-symmetric impact occurs owing to the displacement of the contact surface relative to the symmetric axis of the oval pass, which is demonstrated by the superposition of the graph of $z(\theta)$ dependence on the picture of the deformation zone in the *XY* plane at $\gamma = 35°$, as shown in **Fig. 11**. This leads to the imposition of additional shear in the deformation zone, which substantially affects the stress distribution and the quality of metal processing.

Table 1 Dependence of z_{max} and $\theta_{z.max}$ on the pass inclination angle γ

γ		$\theta_{z.max}$		z_{max}
deg	rad	rad	deg	mm
0	0	0	0	43.53
5	0.087	-0.132	-7.56	43.67
10	0.175	-0.264	-15.13	44.09
15	0.262	-0.4	-22.92	44.81
20	0.349	-0.535	-30.65	45.88
25	0.436	-0.673	-38.56	47.37
30	0.524	-0.815	-46.7	49.41
35	0.611	-0.966	-55.35	52.24
40	0.698	-1.136	-65.09	56.45
45	0.785	-1.362	-78.04	64.33

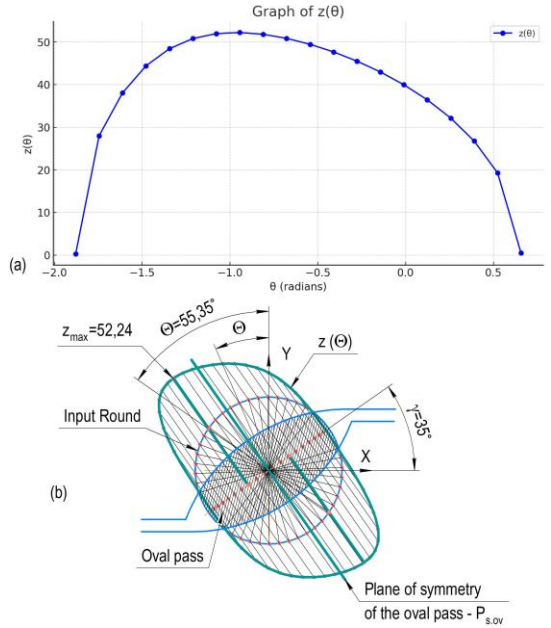

Fig. 11 Imposition of the *z(θ)* plot dependence on the picture of the deformation zone in the *XY* plane at $\gamma = 35°$

In addition, as angle γ increased, z_{max} corresponding to the roll grip length L also increased. The consequence of the increase in the roll grip length L is the expansion of the contact surface area when rolling through inclined oval passes.
Thus, an increase in γ leads to a more complex deformation between the metal and rolls. The results obtained emphasize the necessity of considering these factors when designing passes and selecting rolling parameters to ensure optimal product quality.

Influence of Oval Pass Inclination on Plastic Flow and Stress-Strain State

The results of the numerical modeling of the hot rolling processes show the features of the metal plastic flow in the deformation zone for each pass variant. **Fig. 12** illustrates the distinctive features of the metal flow, as manifested in the formation of symmetric and vortex flows.
In classical oval passes, the formation of metal flows in the transverse direction is mainly due to compression and is directed towards each other with subsequent displacement to the sides, as shown in **Fig. 12a**. Simultaneously, vortex plastic flows were formed in the deformation zone of the inclined oval pass in the cross section, as shown in **Fig. 12b**. The results indicate that the plastic flow of the metal in the inclined oval pass has a nonmonotonic character, in contrast to the more ordered flow observed in classical oval passes. This is owing to the effect of additional shear stresses arising from the specific geometry of the inclined passes. This deformation flow structure has a significant advantage in terms of forming metal properties. For example, [22] argued that non-monotonic metal flow characterizes intense plastic deformations and provides the formation of angular disorientation of boundaries and ultrafine grains with equiaxed shapes.

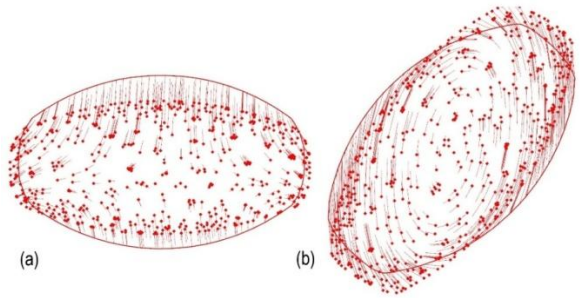

Fig. 12 The picture of the metal plastic flow during rolling in classical (a) and inclined oval passes (b)

Fig. 13 presents the distribution of the effective stress in the deformation zone during workpiece rolling in oval passes. The comparison of two variants of oval passes (the classical oval pass and inclined oval pass) makes it possible to reveal the peculiarities of the formation of the stress state of the metal in the deformation zone.

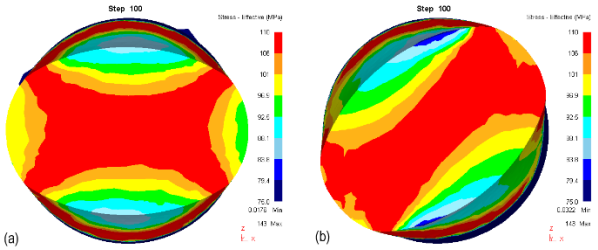

Fig. 13 Effective stress distribution in the deformation zone during rolling in classical (a) and inclined oval passes (b)

When rolling in a classical oval pass, the effective stress distribution exhibited a characteristic symmetrical pattern with the predominance of maximum stress zones in the regions oriented along the longitudinal axis of the workpiece, as shown in **Fig. 13a**. In the case of the inclined oval pass, the stress distribution was significantly different because the high-intensity values covered a wider area, including the lateral zones of the workpiece, as shown in **Fig. 13b**. The broader zone of high stresses in the inclined pass indicates that the metal underwent a more intensive treatment over the entire thickness, which contributed to an improved structure, reduced porosity, and elimination of internal defects, thereby improving the overall quality of the finished rolled product.
A quantitative comparison of the stress state of the metal during rolling in the classical and inclined oval passes involved determining the ratios of stress intensities, which are presented as a histogram in **Fig. 14** and listed in **Table 2**.
Table 2 shows that in the inclined oval pass, the stress distribution exhibited greater homogeneity and a high level of intensity. Thus, the stress range from 80 to 87 MPa is practically absent in the classical oval pass, whereas in the inclined oval pass, it occupies approximately 5%.
The average stress value for both passes was 101 MPa, but the standard deviation was higher for the inclined pass (8.29 vs. 7.83 MPa), indicating a broader range of stress variation. The minimum stress value was also lower for the inclined pass (81.1 vs. 86.2 MPa), whereas the maximum value was higher (118 vs. 116 MPa).
In addition, the share of stress values above 100 MPa in the classical oval pass was 47.5%, whereas it reached 57.7 % in the inclined oval pass. This indicates a higher degree of metal processing in the deformation zone when an inclined oval pass is used, which can improve the quality and mechanical properties of the rolled product.
Analysis of the distribution of accumulated shear strain, presented in **Fig. 15**, reveals minor differences in the characteristics of plastic metal flow during rolling in conventional (a) and inclined (b) oval passes.

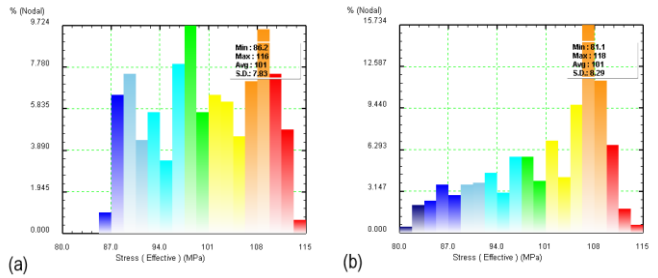

Fig. 14 Histogram of quantitative ratios of effective stress in the deformation zone during rolling in classical (a) and inclined oval passes (b)

Table 2 Quantitative effective stress ratios

Boundaries of effective stress ranges, MPa		**Quantitative ratios, %**	
Lower boundary	Upper boundary	Classical oval pass	Inclined oval pass
80	81.75	0	0.46
81.75	83.5	0	2.14
83.5	85.25	0	2.44
85.25	87	0.99	3.66
87	88.75	6.58	2.9
88.75	90.5	7.57	3.66
90.5	92.25	4.44	3.82
92.25	94	5.76	4.58
94	95.75	3.45	3.05
95.75	97.5	8.06	5.8
97.5	99.25	9.87	5.8
99.25	101	5.76	3.97
101	102.75	6.58	7.02
102.75	104.5	6.25	4.27
104.5	106.25	4.61	9.77
106.25	108	7.24	15.88
108	109.75	9.7	11.6
109.75	111.5	7.57	6.72
111.5	113.25	4.93	1.83
113.25	115	0.66	0.61

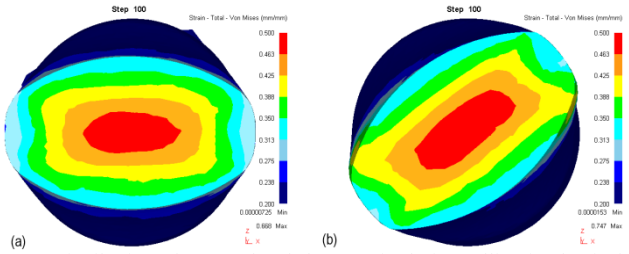

Fig. 15 Distribution of accumulated shear strain during rolling in classical (a) and inclined oval passes (b)

A visual analysis of the distribution of accumulated strain during rolling in a classic oval pass, shown in **Fig. 15a**, demonstrates a symmetrical arrangement of deformation zones with a gradual increase in intensity towards the center of the strip. The maximum values (area highlighted in red) were concentrated in the central part of the workpiece, smoothly transitioning to the less-stressed zones of yellow, green, and blue. The outer layers, indicated by the dark blue color, did not undergo significant deformation.

When rolling in an inclined oval pass, a shift in the zone of maximum accumulated strain towards the direction of plastic flow of the metal was observed. **Fig. 15b** shows that the red zone is more elongated and asymmetrically located relative to the workpiece center. This image indicates a redistribution of stresses and an increase in the intensity of the plastic deformation in some directions. This effect was accompanied by a more pronounced gradient between the high- and low-deformation zones owing to the altered kinematics of the metal flow when using the inclined oval.

To evaluate the intensity and uniformity of plastic deformation during rolling of the workpiece in classical and inclined oval passes, the percentages of different levels of accumulated shear strain degree were determined, which are shown as a histogram in **Fig. 16** and presented in **Table 3**.

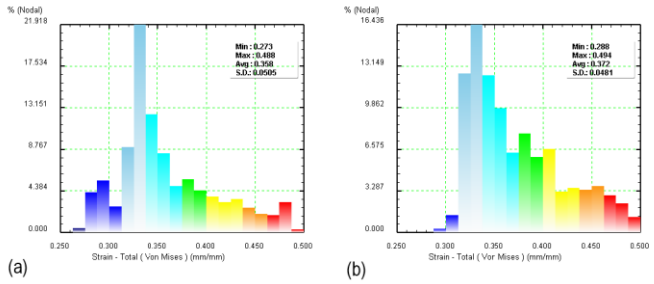

Fig. 16 Histogram of quantitative ratios of the accumulated shear strain degree during rolling in classical (a) and inclined oval passes (b)

Table 3 Quantitative ratios of the accumulated shear strain degree

Boundaries of ranges of accumulated shear strain degree		**Quantitative ratios, %**	
Lower boundary	Upper boundary	Classical oval pass	Inclined oval pass
0.25	0.26	0	0
0.26	0.28	0.46	0
0.28	0.29	4.26	0
0.29	0.30	5.48	0.31
0.30	0.31	2.74	1.38
0.31	0.32	8.98	12.6
0.33	0.34	21.92	16.44
0.34	0.35	12.48	12.44
0.35	0.36	8.37	9.83
0.36	0.38	4.87	6.3
0.38	0.39	5.63	7.83
0.39	0.40	4.41	5.99
0.40	0.41	3.81	6.61
0.41	0.43	3.2	3.23
0.43	0.44	3.5	3.53
0.44	0.45	2.59	3.38
0.45	0.46	1.98	3.69
0.46	0.47	1.83	2.92
0.48	0.49	3.2	2.3
0.49	0.50	0.3	1.23

According to **Table 3**, the maximum value of the accumulated shear strain degree in the classical oval pass was 0.488, and that in the inclined oval pass was 0.494. The average value in the first case is 0.358, whereas that in the second case is 0.372. This difference indicates a greater intensity of strain accumulation when an inclined oval pass is used.

Let us consider the distribution of the percentages of the different ranges of accumulated strain degree. In the range of 0.25-0.30, the classical oval pass showed higher values, reaching a total of 10.2%, whereas the inclined oval pass showed a figure of only 0.31%.

However, for large values of the accumulated strain degree (over 0.40), an opposite trend was observed. In particular, the proportion of values greater than 0.40 in the inclined oval pass was 26.5%, which was 33.8% higher than that in the classical oval pass (19.8%). This indicates that the inclined oval pass provides a more intense deformation than the traditional variant. In addition, the standard deviation of the accumulated strain degree values is 0.0505 for the classical oval pass and 0.0481 for the inclined oval pass. This indicated a smaller dispersion of values in the inclined oval pass, which may indicate a more uniform load distribution during the rolling process.

Experimental Results

The experimental study confirmed the feasibility of rolling circular steel bars using the newly proposed "oval–round" pass design with an inclined oval orientation. Preliminary visual inspection and dimensional measurements of the wire rod samples (**Fig. 17**) showed that the surface was smooth and uniform, the cross-sectional shape was nearly perfectly round, and the dimensions were within the specified tolerances.

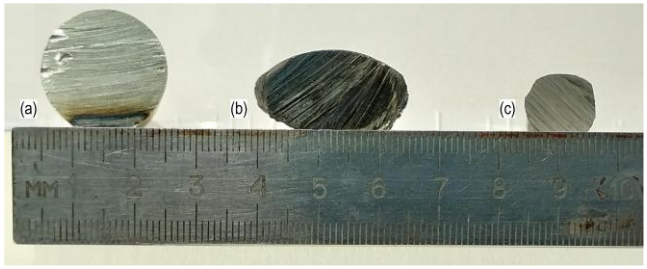

Fig. 17 Cross-sections of samples: (a) initial, (b) after one pass, and (c) after four passes of rolling using the new "oval–round" pass design

Tensile tests conducted according to ISO 6892-1 provided stress–strain curves for the initial material and samples rolled through both the classical and the new "oval–round" schemes. **Fig. 18** presents a typical stress–strain curve for a sample rolled using the new pass design. The diagram illustrates the usual behavior of steel under uniaxial tension, including the elastic region, yield point, strain hardening, and fracture. Similar curve shapes were observed for samples rolled using the classical method, indicating a comparable material response under tensile loading.

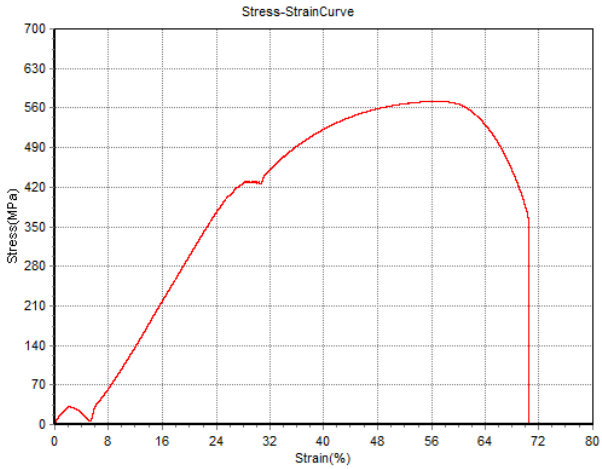

Fig. 18 Stress–strain curve obtained during tensile testing of a 25G2S steel specimen rolled using the new "oval–round" pass sequence.

Table 4 presents the average strength and ductility characteristics of the 25G2S steel samples. The results reveal a significant increase in strength for both rolling methods: the yield strength increased from 273.4 MPa to 437.8 MPa (classical scheme) and 432.2 MPa (new scheme), while the ultimate tensile strength increased from 493.8 MPa to 583.5 MPa and 573.3 MPa, respectively. Notably, the new scheme led to an improvement in ductility characteristics: elongation at break increased to 26.1% (compared to 22.6% in the classical scheme), and reduction of area reached 69.2% (compared to 66.0%).

This outcome is especially important in the context of the well-known strength–ductility trade-off, where enhancing one property usually compromises the other. As highlighted by Zhang et al. [23], "Strength and ductility are always in opposition, i.e., improving one is usually at the expense of the other." However, with the new "oval–round" pass design, this conflict appears to be partially alleviated: strength parameters have increased compared to the initial material, without the typical loss in ductility; conversely, ductility has improved compared to the classical rolling scheme.

Thus, the proposed rolling scheme with inclined oval passes not only enables more intensive plastic deformation by engaging a larger metal volume—as demonstrated by numerical simulations and stress/strain distribution analysis—but also achieves a more favorable balance between strength and ductility. This makes the new approach a promising candidate for industrial applications that aim to enhance product quality and performance.

Table 4 Average Strength and Ductility Characteristics of 25G2S Steel Samples

Sample	Yield strength, MPa	Ultimate tensile strength, MPa	Elongation at break, %	Reduction of area, %
Initial (unrolled)	273.4	493.8	23.3	63.3
After rolling with classical "oval–round" pass design	437.8	583.5	22.6	66.0
After rolling with new "oval–round" pass design	432.2	573.3	26.1	69.2

Future research directions will include a detailed analysis of the influence of the new "oval–round" rolling scheme on the micromechanical properties of the material. This will involve comprehensive metallographic studies aimed at examining the evolution of the microstructure, grain refinement, phase transformations, and defect distribution induced by the enhanced shear deformation. Particular attention will be paid to correlating these microstructural changes with the observed improvements in mechanical performance.

As one promising avenue for future development, we plan to explore the integration of thermomechanical processing with macro-shear deformation, aiming to combine controlled thermal treatment with deformation-induced microstructural refinement in a synergistic manner. This approach is supported by findings from Kvackaj et al. [24], who demonstrated that reheating conditions, specifically temperature and holding time, have a significant impact on austenite grain size and its evolution—parameters that in turn critically influence the final microstructure and material properties.

CONCLUSION

Based on the theoretical development, numerical analysis, and experimental validation of the oval–round pass design for intensified shear deformation in rod rolling, the following conclusions can be drawn:

1. A method for implementing intensive shear deformations during rolling in an oval-round pass design, owing to the inclined arrangement of the oval passes relative to the roll axis, was developed and substantiated.
2. The proposed four-pass rolling scheme, which provides alternating shear directions, makes it possible to implement alternating macro shear deformation.
3. The results of the analytical determination of the roll grip length during rolling in inclined oval passes agreed with the results of the 3D modeling, which confirmed the accuracy of the proposed model.
4. Numerical modeling showed vortex flows of metal plastic flow and more extensive zones of high stresses in inclined oval passes, indicating the active involvement of material volume in the deformation process.
5. The distribution of the accumulated degree of shear deformation in the inclined passes has a greater intensity and uniformity than that in the classical passes, which indicates an increased effectiveness of hardening and improvement of the metal structure.
6. The experimental results confirmed that the new inclined oval–round pass design allows for a more favorable combination of strength and ductility in rolled products, partially overcoming the strength–ductility trade-off.
7. The use of inclined oval passes contributed to better surface quality, dimensional accuracy, and microstructural refinement of the rolled steel.
8. Future studies will be directed at detailed metallographic analysis to evaluate the microstructure evolution, grain refinement, and defect elimination mechanisms facilitated by the intensified shear deformation.

Acknowledgements: This research has been funded by the Science Committee of the Ministry of Science and Higher Education of the Republic of Kazakhstan (Grant No. AP19674502).

REFERENCES

1. L.S. Bayoumi: International Journal of Mechanical Sciences, 40(12), 1998, 1223–1234. https://doi.org/10.1016/S0020-7403(98)00005-8
2. L.S. Bayoumi, Y. Lee: Journal of Materials Processing Technology, 145(1), 2004, 7–13. https://doi.org/10.1016/S0924-0136(03)00581-8
3. B. Huang, K. Xing, K. Abhary, S. Spuzic: Robotics and Computer-Integrated Manufacturing, 28(4), 2012, 493–499. https://doi.org/10.1016/j.rcim.2012.02.004
4. J.-K. Hwang: Materials Science and Engineering: A, 707, 2017, 1–9. https://doi.org/10.1016/j.msea.2017.11.031
5. A. Schowtjak, S. Wang, O. Hering, T. Clausmeyer, J. Lohmar, R. Schulte, R. Ostwald, G. Hirt, A.E. Tekkaya: Production Engineering, 13(1), 2019, 1–9. https://doi.org/10.1007/s11740-019-00935-x
6. J. Hába, R. Fabík: Optimizing of the degree of elongation in a single pass during hot workpieces rolling in the oval-round roll pass schedule. In *Proceedings of METAL 2016,* Brno, Czech Republic, 25–27 May 2016, p. 285-290. https://www.confer.cz/metal/2016/read/1747
7. E.M. Zayed, A. El-Sabbagh, N.A. El-Mahallawy, M. Shazly: Heliyon, 9(6), 2023, e16700. https://doi.org/10.1016/j.heliyon.2023.e16700
8. E. Bagherpour, N. Pardis, M. Reihanian, H.S. Kim: International Journal of Advanced Manufacturing Technology, 100(5–8), 2019, 1647–1694. https://doi.org/10.1007/s00170-018-2652-z
9. P. Dolzhenko, M. Tikhonova, M. Odnobokova, R. Kaibyshev, A. Belyakov: Metals, 13(4), 2023, 674. https://doi.org/10.3390/met13040674
10. V. Segal: Materials Science and Engineering: A, 338(1–2), 2002, 331–344. https://doi.org/10.1016/S0921-5093(02)00066-7
11. V. Segal: Materials, 11(7), 2018, 1175. https://doi.org/10.3390/ma11071175
12. J. Bidulska, et al.: Chemicke Listy, 105(SI4), 2011, S471-S473.
13. A.B. Naizabekov, M.B. Bykhin, K.A. Nogaev, B.B. Bykhin: Study of the process of realization of high-rate plastic deformation in lengthwise rolling. In *Proceedings of METAL 2010*, Brno, Czech Republic, 18–20 May 2010, p. 192-202. https://www.confer.cz/metal/2010
14. M. Abishkenov, Z. Ashkeyev, K. Nogaev: Materialia, 26, 2022, 101573. https://doi.org/10.1016/j.mtla.2022.101573
15. Z. Ashkeyev, M. Abishkenov, K. Nogaev, Y. Bestembek, K. Azimbayev, I. Tavshanov: Engineering Solid Mechanics, 11(3), 2023, 253–262. https://doi.org/10.5267/j.esm.2023.3.004
16. Y. Dong, J. Song, G. Luo, Z. Ren: International Journal of Mechanical Sciences, 115–116, 2016, 180–189. https://doi.org/10.1016/j.ijmecsci.2016.03.021
17. R.R. Dema, V.V. Alontsev, O.B. Kalugina, A.N. Shapovalov: Materials Today: Proceedings, 19(5), 2019, 2312–2315. https://doi.org/10.1016/j.matpr.2019.07.677
18. A. Kumar, S. Rath, M. Kumar: Materials Today: Proceedings, 42(2), 2020, 650–659. https://doi.org/10.1016/j.matpr.2020.11.050
19. Z. Pater, J. Tomczak, T. Bulzak: Archives of Civil and Mechanical Engineering, 18(1), 2018, 149–161. https://doi.org/10.1016/j.acme.2017.06.005
20. F. Baciu, A. Rusu-Casandra, S.D. Pastramă: Materials Today: Proceedings, 32(2), 2020, 128–132. https://doi.org/10.1016/j.matpr.2020.03.469
21. T.H. Cormen, C.E. Leiserson, R.L. Rivest, C. Stein: *Introduction to Algorithms,* 4th ed., Cambridge, MA: The MIT Press, 2022.
22. A.M. Pesin, D.O. Pustovoytov, T.V. Shveeva, V.L. Steblyanko, S.A. Fedoseev: Vestnik of Nosov Magnitogorsk State Technical University, 15(1), 2017, 56–63. http://dx.doi.org/10.18503/1995-2732-2017-15-1-56-63
23. C. Zhang, H. Yu, S. Antonov, W. Li, J. He, H. Zhi, Y. Su: Corrosion Science, 207, 2022, 110579. https://doi.org/10.1016/j.corsci.2022.110579
24. T. Kvackaj, J. Bidulská, R. Bidulský: Materials, 14(8), 2021, 1988. https://doi.org/10.3390/ma14081988